ARTICLE OPEN

Check for updates

Individualized identification value of stress-related network structural-functional properties and HPA axis reactivity for subthreshold depression

Youze He[1,2,4], Baoru Zhao[1,4], Zhihan Liu[1,4], Yudie Hu[1], Jian Song[1,2] and Jingsong Wu[1,3]✉

Accumulating studies have highlighted the links between stress-related networks and the HPA axis for emotion regulation and proved the mapping associations between altered structural and functional networks (called SC-FC coupling) in depression. However, the signatures of SC-FC coupling in subthreshold depression (StD) individuals and their relationships with HPA axis reactivity, as well as the predictive power of these combinations for discriminating StD, remain unclear. This cross-sectional study enrolled 160 adults, including 117 StD and 43 healthy controls (HC). The propensity score matching method was applied for match-pair analysis between StD and HC. Herein, we measured depression level, cortisol level, and brain imaging outcomes. The functional MRI and diffusion tensor imaging methods were employed to acquire the network SC-FC couplings and topological attributes. Support vector machine models were employed to discriminate StD from HC. Herein, 43 pairs were matched, but four participants were excluded due to over-threshold head motion, leaving 41 participants in each group. General linear model results revealed a significant SC-FC coupling increase in the default mode network (DMN) and decrements of global efficiency in DMN and frontoparietal control network ($P < 0.05$), while the cortisol secretion significantly increased ($P < 0.001$) in StD individuals. Partial correlation analysis revealed positive associations between DMN coupling and cortisol values ($r = 0.298$, $P = 0.033$), and their combination provided greater power for discriminating StD than another single model, with the classification accuracy and AUC value up to 85.71% and 0.894, respectively. In summary, this study clarified the relationship between stress-related network SC-FC coupling and cortisol secretion in influencing depressive symptoms, whose combination would contribute to discriminating subthreshold depressive states in the future.

Translational Psychiatry (2024)14:501 ; https://doi.org/10.1038/s41398-024-03210-5

INTRODUCTION

Subthreshold depression (StD) individuals undergo two or more depressive symptoms without reaching major depressive disorder (MDD) diagnostic criteria [1, 2]. A recent meta-analysis estimated the prevalence of StD to be 11.02% [3]. Despite not meeting the full criteria of MDD, StD individuals often experience chronic fatigue, memory impairment, insomnia, and poor concentration, all of which can significantly affect their quality of life and increase their risk of suicide risk [4, 5]. Therefore, understanding the underpinning mechanism and recognition of StD can aid in the prevention of depression.

Accumulating evidence has demonstrated that high-level stress is a major threat to the onset and development of subthreshold depression and depression [6]. When perceiving the stressors, the hypothalamic-pituitary-adrenal (HPA) axis was activated to release stress-related hormones, such as corticotropin-releasing hormone and cortisol, to cope with the high-level perceived stress [7]. It was proved that the HPA axis was dysregulated in the pathophysiology of depression-related disorders [8, 9]. One of the primary theories proposed for the HPA axis in depression was that elevated cortisols interfere with glucocorticoid receptor-mediated negative feedback and excitatory toxicity [10]. The elevated circulating cortisol could potentially inhibit neurogenesis in stress-related networks and key nodes that are rich in glucocorticoid receptors, such as the default mode network, frontoparietal network, and salience network [11, 12].

Previous observations in StD individuals showed impaired functional connectivity within the frontoparietal network and enhanced default network connectivity [13, 14]. Neuroimaging studies also identified structural loss in these networks in young StD individuals [15]. Anatomically, structural connectivity imposes a constraint on functional connectivity, which in turn influences structural connectivity through cerebral plasticity [16, 17]. The interplay between structural and functional connectivity is called structural-functional coupling (SC-FC coupling). It could provide more information about the underlying workings of the brain than either feature alone and detect subtle pathological abnormalities more sensitively [18–20]. Notably, previous studies of depression-related disorders (MDD and post-stroke depression) have highlighted the significant loss of SC-FC coupling and disrupted

[1]College of Rehabilitation Medicine, Fujian University of Traditional Chinese Medicine, Fuzhou, China. [2]The Academy of Rehabilitation Industry, Fujian University of Traditional Chinese Medicine, Fuzhou, China. [3]Fujian Key Laboratory of Cognitive Rehabilitation, Affiliated Rehabilitation Hospital of Fujian University of Traditional Chinese Medicine, Fuzhou, China. [4]These authors contributed equally: Youze He, Baoru Zhao, Zhihan Liu. ✉email: jingsongwu01@163.com

Received: 25 May 2024 Revised: 4 December 2024 Accepted: 16 December 2024
Published online: 23 December 2024

topology in the global network that correlated with depressive symptoms [21, 22]. These findings underscored the mechanism underlying depression pathophysiology from the perspective of global network SC-FC coupling. Recently, the macroscale SC-FC couplings have been demonstrated to differ across the cortex and subcortex [23]. And the brain subnetwork SC-FC couplings exhibit diverse changes due to respective network functions in psychiatric disorders [24], revealing the importance of further exploring subnetwork SC-FC coupling changes.

Herein, we would like to specify the distinctive characteristics of different brain networks' SC-FC coupling and examine the associations between cortisol levels and specific brain networks involved in emotional regulation in StD individuals. Additionally, we utilized support vector machine models with the Gaussian kernel method to assess the potential of their combinations as biological markers for distinguishing subthreshold depression from healthy adults. In this study, we hypothesized that (1) StD individuals have unique SC-FC coupling traits in stress-related networks, potentially linked to elevated cortisol levels; and (2) combining network SC-FC coupling traits and cortisol levels can provide strong predictive capabilities for distinguishing StD from HC individuals.

METHODS AND MATERIALS

Participants and procedures

This study was conducted in a cross-sectional study design that enrolled 160 participants, including 117 adults with subthreshold depression (StD) and 43 healthy control (HC) subjects. This research received approval from the Ethics Committee of Rehabilitation Hospital Affiliated with Fujian University of Traditional Chinese Medicine (No.2019KY-003-01) and was conducted in accordance with the Declaration of Helsinki. The study protocol was registered in the Chinese Clinical Trial Registry (Registration number: ChiCTR1900028289). Participants were recruited from the local universities and communities in Fuzhou City, China, via online posters from December 2019 to December 2021.

Eligible participants were aged 18–44, with no gender restriction. In the StD group individuals had to meet the diagnosis criteria of subthreshold depression according to Judd et al., have no major depression or suicidal tendency based on the DSM-V and Mini International Neuropsychiatric Interview (MINI version 5.0), obtain a Center for Epidemiologic Studies Depression Scale (CES-D) score of 16 or higher, have no history of antidepression treatment in the past 6 months, and have no MRI contraindications. For the HC group, inclusion criteria included having a CES-D score of less than 16 and having no MRI contraindication. Exclusion criteria for both groups involved meeting the diagnosis criteria of MDD, bipolar disorders, and psychosis based on DSM-V, usage of psychiatric medication or addiction disorder, as well as having any significant medical, neurological, or psychological illness or history of head trauma. Written informed consent was obtained from all participants.

Measures

We used several measures in this study to assess depression, anxiety, and stress levels among the subjects. These measures include the Hamilton Depression Scale (HAMD), Generalized Anxiety Disorders (GAD-7), and Perceived Stress Scale (PSS). The HAMD scale is a widely used clinical measurement for depressive symptoms, which is a sensitive indicator of the severity of depressive symptoms, with higher scores indicating greater depression [25]. The GAD-7 is a self-rating scale used to assess anxiety status, whose scores range from 0 to 21, with higher scores indicating more severe anxiety [26]. The PSS-14 scale Chinese version is used to evaluate the perceived stress levels, which consists of 14 items, with each item scoring from 0 to 4, with higher scores indicating higher levels of stress perception [27].

MRI data collection and processing

MRI data collection and scanning parameters. All participants completed the brain fMRI scanning in the following multi-model sequence. The structural T1 image: weight-sequence in the sagittal plane, repetition time = 2000 ms, echo time = 1.73 ms, field of view = 240 × 240 mm, flip angle = 15°, 1 mm slice thickness with 160 slices, matrix size = 256 × 256. The resting-state image: EPI sequence, repetition time = 2000 ms, echo time=30 ms, flip angle = 90°, field of view = 230 × 230 mm, 3.6 mm slice thickness with 37 slices, matrix =64 × 64, Voxel size=3.6×3.6×3.9 mm^3. The diffusion tensor image: repetition time = 5000 ms, echo time = 69 ms, flip angle = 90°, field of view = 230 × 230 mm, 3.5 mm slice thickness with 35 slices, matrix =64 × 64, Voxel size = 1.8 × 1.8 × 3.5 mm^3.

Preprocessing of MRI data and construction of connection matrix. The resting-state and diffusion tensor images were preprocessed on the Matlab 2020a platform using the GRETNA (https://www.nitrc.org/projects/gretna) software and PANDA software (https://www.nitrc.org/projects/pamda). Preprocessing of the resting-state image involved the following steps: removal of the first ten time points, slice timing, realignment, co-registration, segment, spatial normalization, full width at half maximum of 6 mm for smoothing, and filtering between 0.01 and 0.1 Hz. Preprocessing of the diffusion tensor image included skull removal, cropping gap at 3.0 mm, generation of dispersion matrix parameters (seven voxels), normalization using the FMRIB58_FA template, and smoothing. The brain was divided into 300 nodes based on the Schaefer-300 atlas [28], with 150 nodes in each of the left and right sides of the brain, involving seven subnetworks, including default mode network (DMN), dorsal Attention network (DOR), executive control network (FPC), limbic network (LIM), ventral attention network (VEN), visual network (VIS), and somatomotor network (SOM) [28].

Analysis of structural-functional couplings and topological attributes in multiscale networks. The non-zero structural connections as well as positive functional connections were included in the analysis of this study. Pearson correlation analysis was performed between the structural and functional connectivity matrices for each subject to obtain correlation coefficients representing the strength of structural-functional coupling. Network topological properties were analyzed using the GRETNA software to calculate global and nodal topological properties for each binary network state. To obtain a full picture of the neural changes and avoid bias from a single threshold, this study examined the topological property within a wide sparsity range of 5 to 50% (step 1%) [29]. Topological properties analyzed in this study comprised global properties such as global efficiency, clustering coefficient, and characteristic path length, as well as nodal properties such as nodal efficiency and degree centrality.

Measures of HPA axis activities: Salivary cortisol

Saliva samples were collected from each participant at four time points immediately after awakening: time point 1 (0 min), time point 2 (30 min), time point 3 (45 min), and time point 4 (60 min). Before collection day, participants were provided with four Salvette saliva tubes (Sarstedt, Italy) by staff and instructed to avoid eating, drinking, brushing their teeth, smoking, or exercising until the sample collection was complete. The Salivary Cortisol Enzyme-Linked Immunosorbent Assay Kit (DRG Diagnostics, Germany) was used to analyze the cortisol concentration in the salivary sample. In this study, we calculated the salivary cortisol levels using two metrics: the Area Under the Curve relative to the ground (AUCg) and the Area Under the Curve with respect to increase (AUCi), which represent the total amount of cortisol secreted after awakening and the dynamic changes in cortisol levels following awakening, respectively, based on the formula proposed by Pruessner et al. [30].

Statistical analysis

Statistical analyses were conducted using SPSS software version 24.0. To balance the demographic characteristics between the StD group and the HC group, we utilized the propensity score matching (PSM) method. Covariates used for matching included ages, sex, educational years, and/or BMI with a matching tolerance of 0.02. In this study, the continuous variables such as age, educational years, and testing scale scores were presented as mean (standard deviation) or median (P25, P75) depending on the normality of data distribution and examined the differences between groups using the independent t-test or Mann-Whitney U-tests. The absences of salivary cortisol measurements at time point 3 and time point 4 of two healthy control individuals were encountered. Considering the negligible proportion of missing data, not exceeding 5%, we employed the multiple imputation method to deal with the missing data, thereby preserving the completeness and reliability of our data set [31]. General

Table 1. Demographic information and measures of neuropsychological tests.

	StD Group ALL (N = 117)	Match-paired comparison		t/Z/χ^2	P
		StD (N = 41)	HC (N = 41)		
Age (years)	19.00 (18.00, 20.00)	19.00 (19.00, 20.00)	19.00 (18.00, 20.00)	1.262 [a]	0.207
Sex (Male/Female)	44/73	15/26	16/25	0.052 [b]	0.820
BMI (Kg/m^2)	20.98 (18.63, 23.95)	20.81 (18.81, 23.27)	20.55 (18.91, 23.31)	0.450 [a]	0.653
Educational years	14.00 (13.00, 14.00)	14.00 (13.00, 14.50)	13.00 (13.00, 14.50)	1.598 [a]	0.110
CESD	20.00 (16.00, 27.00)	19 (17.00, 23.00)	6.00 (3.00, 11.00)	7.807 [a]	<0.001
MoCA	29.00 (28.00, 30.00)	29.00 (28.00, 30.00)	29.00 (28.00, 30.00)	0.554 [a]	0.580
HAMD	9.00 (7.00, 11.50)	9.00 (7.00, 11.00)	3.00 (0.00, 5.50)	5.973 [a]	<0.001
GAD7	7.00 (4.00, 10.00)	6.00 (5.00, 9.50)	2.00 (1.00, 5.00)	4.645 [a]	<0.001
PSS	29.00 (25.00, 34.00)	28.90 ± 6.61	22.88 ± 8.61	−3.556 [c]	0.001

[a]The Mann–Whitney U test was applied due to the non-normal distribution of the continuous variable;
[b]The chi-square test was applied for the categorical variable;
[c]The independent t-test was employed due to the normal distribution of the continuous variable.

linear model (GLM) analysis was used to compare the group differences in brain network structure-function coupling and topological properties. We controlled for age and sex as covariates in this analysis. Additionally, partial correlation analyses were conducted to explore the associations among clinically negative symptoms and brain network structure-function couplings and topological attributes. Statistical significance was determined at a P value less than 0.05 (uncorrected).

To classify the StD and HC individuals, we applied SVM with the Gaussian kernel method to separately achieve classification accuracy, sensitivity, specificity, F1 values, and AUC values using the R software 4.3.1 version. These values were estimated by the simple cross-validation method with 80% participants for the training sets and 20% participants for the testing sets. Due to the significant group differences in DMN network characteristics and salivary cortisol levels, we included these variables in the SVM models, respectively, and constructed the four SVM models in addition to the basic variables (age, sex, educational years, and HAMD scores).

RESULTS

Demographics and outcomes between StD and HC and between sex subgroups

A total of 82 participants were included in the final analysis, with 41 participants in both the StD and HC groups. Initially, a total of 43 StD individuals were matched with the HC group based on age, sex, and educational years. However, four participants were excluded due to over-threshold head motion, with two individuals from each group. The MRI head motion parameters (the mean translation and rotation in the X, Y, and Z axes as well as the mean FD_Jenkinson score) of the remaining individuals in both groups were not significant ($P > 0.05$) (See Supplementary Table S1).

There were no significant demographic differences between the StD group and HC group in terms of age, sex, educational years, BMI, or MoCA score ($P > 0.05$). Concerning emotional symptoms, statistically significant differences were observed between the StD group and HC group for CES-D scores ($P = 0.001$), HAMD scores ($P = 0.001$), PSS scores ($P = 0.001$), and GAD-7 scores ($P = 0.001$) (See Table 1).

Difference of SC-FC coupling between StD and HC

The comparison of SC-FC coupling of the seven networks was conducted between the StD group and HC group and between sex subgroups of StD individuals. The GLM analysis of SC-FC coupling revealed a significant difference in the SC-FC coupling of the DMN network ($t = -2.217$, $P = 0.030$) between the StD and HC group (See Fig. 1A), while no significant between-group difference in the DOR, FPC, LIM, SOM, VEN, and VIS networks (See Supplementary Table S2).

Difference of global topological attributes between StD and HC groups

Due to the significant difference in SC-FC coupling between the StD individuals and HC groups, we further investigate the within-network characteristics in view of the functional and structural network global topological attributes. In terms of functional networks, the DMN and FPC network global efficiency of StD individuals were significantly decreased ($t = 2.026$, $P = 0.046$; $t = 3.011$, $P = 0.004$, respectively) when compared to the HC group after controlling for age and sex variable (See Fig. 1B, C and Supplementary Table S3). Besides, the FPC network characteristic path length was significantly increased ($t = -3.382$, $P = 0.001$) after controlling for these covariates (See Fig. 1D and Supplementary Table S4). However, no significant between-group differences were found in the functional clustering coefficient, structural global efficiency, structural characteristic path length, and structural clustering coefficient in these seven networks ($P > 0.05$) (See Supplementary Tables S5–8).

Difference of nodal topological attributes within the DMN and FPC networks between StD and HC groups

To further explore the subtle changes within the network accompanied by functional global changes, we conducted the comparison of nodal topological attributes in DMN and FPC networks between the StD and HC groups. Our results showed that the StD individuals exhibited significant increases in degree centrality of the left Temporal lobe (Temp), posterior cingulate cortex (PCC), and increases in nodal efficiency of the left PCC in the functional DMN network ($P < 0.05$, Bonferroni correction). Besides, there were significant decreases in degree centrality and nodal efficiency of the right dorsal medial prefrontal cortex (dmPFC) ($P < 0.05$, Bonferroni correction) (See Fig. 1H).

Regarding the functional FPC network, the StD individuals demonstrated significant decreases in degree centrality and nodal efficiency of the lateral prefrontal cortex (PFCl) ($P < 0.05$, Bonferroni correction). There was also a significant increase in the right precuneus nodal degree centrality when compared to the HC group ($P < 0.05$, Bonferroni correction) (See Fig. 1I).

Differences in salivary cortisol secretion between StD and HC group

Both StD and HC participants showed increases in salivary cortisol secretion from time point 1 (0 min after waking up) to time point 2 (30 min after waking up), followed by a decreasing trend from time point 2 to time point 3 (45 min after waking up) and time point 4 (60 min after waking up). There were significant differences between StD and HC groups at time point 1

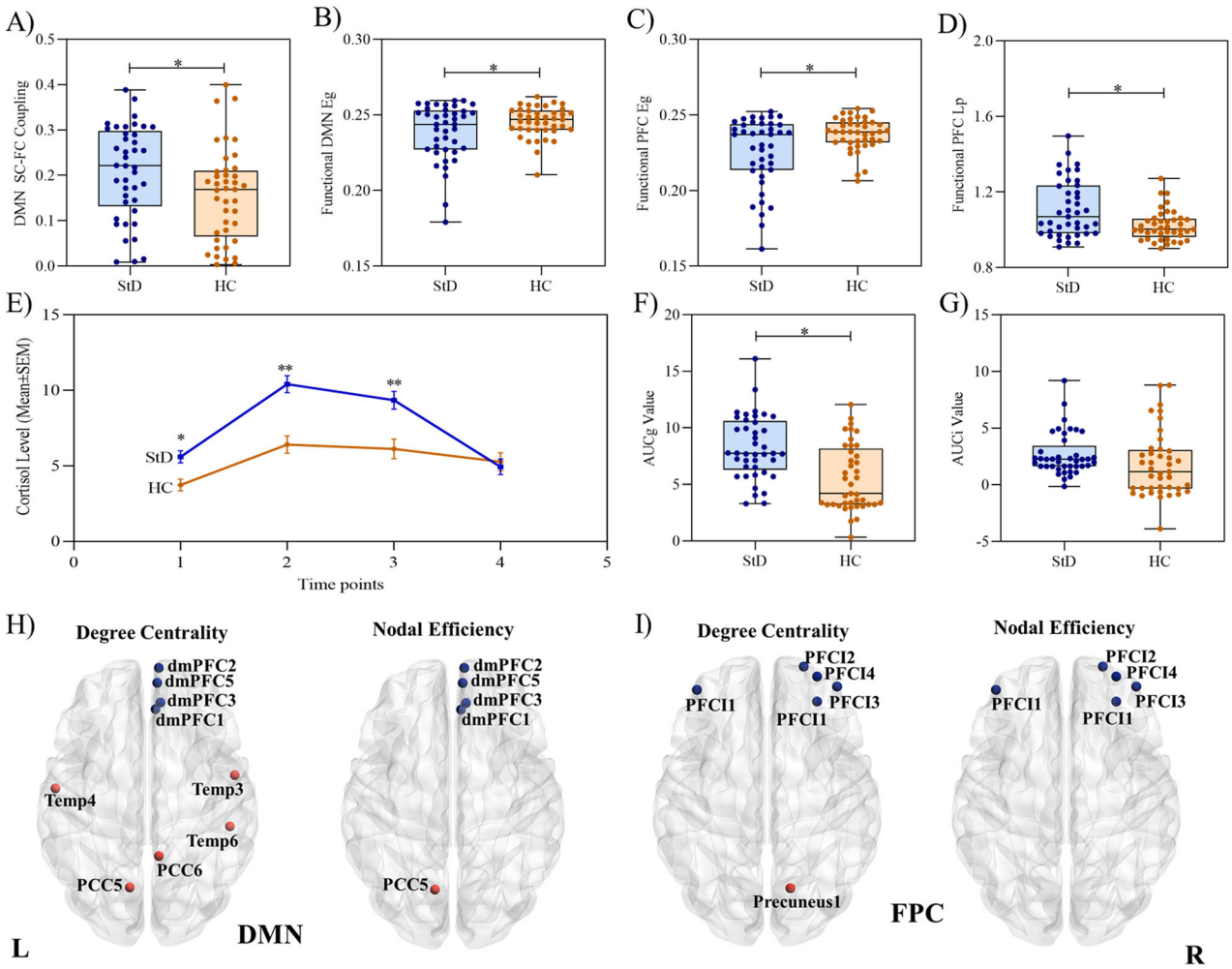

Fig. 1 Comparison of group differences in measured outcomes. Comparisons of networks' SC-FC couplings, cortisol levels, and nodal topological characteristics. **A** Differences in DMN network structural-functional (SC-FC) couplings between groups; **B** differences in functional DMN network global efficiency (Eg) between groups; **C** differences in functional FPC network global efficiency between groups; **D** differences of functional FPC network characteristic path length (Lp) between groups; **E** differences in cortisol secretion levels between groups over four-time point after awaken up; **F** differences in area under the curve relative to the ground (AUCg) between groups; **G** differences in area under the curve with respect to increase (AUCi) between groups; **H** differences in degree centrality and nodal efficiency within the DMN network between groups; **I** differences in degree centrality and nodal efficiency within the FPC network between groups.

($P = 0.002$), time point 2 ($P < 0.001$), and time point 3 ($P < 0.001$) (Fig. 1E and Supplementary Table S9). Furthermore, the AUCg values were significantly higher in StD individuals than in HC individuals ($P < 0.001$), while there was no significant difference in AUCi values between groups ($P > 0.05$) (Fig. 1F, G and Supplementary Table S9).

Partial correlation analysis

The partial correlation analyses revealed significant associations between the DMN network's SC-FC coupling values and CES-D scores ($r = 0.420$, $P = 0.008$) (See Fig. 2A). The StD individuals also exhibited significant negative correlations between HAMD scores and degree centrality of right dmPFC ($r = -0.461$, $P = 0.003$) and right PFCL ($r = -0.464$, $P = 0.003$), as well as nodal efficiency of right dmPFC ($r = -0.420$, $P = 0.008$) and right PFCL ($r = -0.427$, $P = 0.007$) (See Fig. 2B–E). Furthermore, the AUCg values were significantly correlated with DMN SC-FC couplings in StD individuals ($r = 0.298$, $P = 0.033$) (See Fig. 2F).

Classification of support vector machine (SVM)

The SVM results showed the classification accuracy, sensitivity, specificity, and F1 score up to 76.47%, 85.71%, 70.00% and 0.750 based on the DMN SC-FC coupling values in the model 1; 78.57%, 71.43%, 85.71% and 0.769 based on the functional dmPFC nodal efficiency and degree centrality in the model 2; 66.67%, 63.64%, 71.43% and 0.700 based on the salivary cortisol level in the model 3; and 85.71%, 84.62%, 87.50%, and 0.880 based on the combination of DMN SC-FC coupling values and salivary cortisol level in the model 4 (See Table 2). Moreover, the AUC values in these four models presented values of 0.871, 0.837, 0.766, and 0.894, respectively (See Table 2 and Fig. 3). These findings indicated that the combination of DMN SC-FC coupling values and salivary cortisol level provided better power for discriminating the StD individuals from the HC individuals.

DISCUSSION

This study clarified the brain network SC-FC coupling and inner topological characteristics in StD adults and first employed the combination of brain activity and HPA axis activities for early discrimination of subthreshold depression. The findings suggested that the DMN network exhibited increased SC-FC couplings, along with decreased functional global efficiency, while the FPC

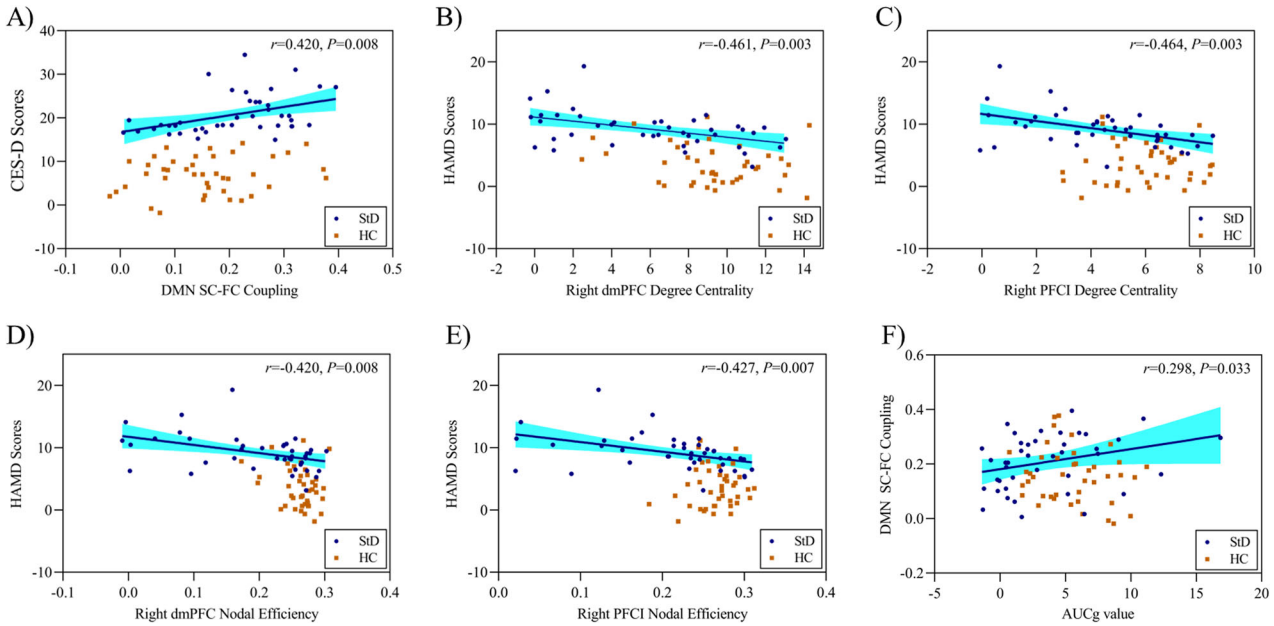

Fig. 2 The correlations analysis results among measured outcomes. The partial correlation analyses were conducted for (**A**–**F**), adjusting age and sex variables. **A** Correlations between CES-D scores and the DMN network structural-functional (SC-FC) coupling; **B** correlations between HAMD scores and degree centrality of the right dorsal medial prefrontal cortex (dmPFC); **C** correlations between HAMD scores and degree centrality of the right lateral prefrontal cortex (PFCI); **D** correlations between HAMD scores and nodal efficiency of the right dmPFC; **E** correlations between HAMD scores and nodal efficiency of the right PFCI; **F** correlations between the DMN network SC-FC coupling and the area under the curve relative to the ground (AUCg) value. The blue circle represents the subthreshold depression group (StD) and the orange square represents the healthy control group (HC).

Table 2. Results of four included SVM models.

	Accuracy	Sensitivity	Specificity	F1 score	AUC
Model 1	76.47%	85.71%	70.00%	0.750	0.871
Model 2	78.57%	71.43%	85.71%	0.769	0.837
Model 3	66.67%	63.64%	71.43%	0.700	0.766
Model 4	85.71%	84.62%	87.50%	0.880	0.894

Basic variables included age, sex, educational years, and HAMD scores; Model 1: Included basic variables and the DMN network SC-FC coupling; Model 2: Included basic variables and the dmPFC node efficiency and degree centrality; Model 3: Included basic variables and salivary cortisol; Model 4: Included basic variables, salivary cortisol, and the DMN network SC-FC coupling.

functional network showed decreased global efficiency. Further explorations through graph theory identified subtle changes in degree centrality and nodal efficiency within these networks. Herein, we also found a significant correlation between cortisol secretion level and DMN coupling, and their combination performed the greater power than other single models in discriminating subthreshold depression from healthy controls.

Previous literature supported the notion that networks with protracted development, such as DMN and salience networks, exhibited relatively weak SC-FC coupling in healthy individuals [32, 33]. In the emotional regulation process, the DMN network played crucial roles in generating affective states via modulation of autonomic and endocrine activity and impacted affect-based decision-making, understanding of affective cues, and perceptions of valence in facial expressions [34]. In the StD individuals, this study revealed increased DMN network SC-FC coupling that correlated with depressive symptoms, which might represent more needs for DMN network information interaction for StD individuals to maintain emotional regulation ability. This phenomenon was in line with previous findings of enhanced DMN network connectivity in StD individuals [14]. Additionally, recent static SC-FC coupling work has quantified temporal fluctuations across time. It pointed out that transmodal regions across DMN, FPC, and limbic network displayed more fluctuations than unimodal regions and the brain regions occupying intermediated positions displayed the greatest fluctuations [23]. Hence, this study employed the graph theory analysis to further explore the inner changes of the DMN network. Our findings revealed the decrements of degree centrality and nodal efficiency in the dmPFC while increments of PCC regions in StD individuals, which were in line with previous findings in depressed patients [35, 36]. As key hubs within the DMN network, the dmPFC functions in self-referential processing and social cognition, while the PCC works for episodic memory retrieval, emotional processing, and self-referential processing [37]. Compared with dmPFC, the PCC plays more role in information interaction with other networks and cross-mode connection [38]. Hence, the enhanced connections of PCC in StD individuals were more likely to affect the DMN SC-FC coupling fluctuation and might contribute more to the increment of DMN network SC-FC coupling to some extent.

Moreover, this study found lower global efficiency of the FPC network in StD individuals compared to healthy controls, as well as reduced degree centrality and nodal efficiency of the lateral prefrontal cortex, which indicate decreases in information transmission ability and functional activation of the FPC network. This phenomenon in StD individuals is similar to that in MDD

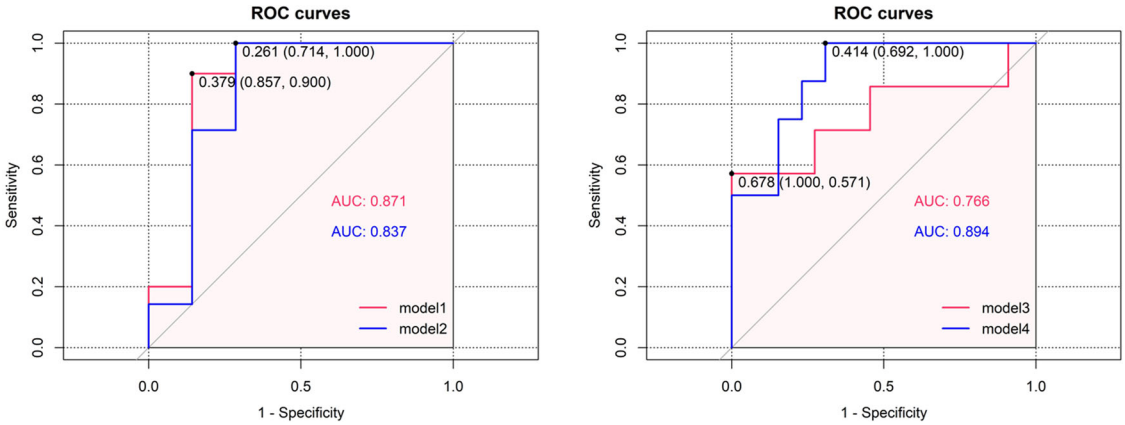

Fig. 3 ROC curves of SVM models.

patients. For instance, a meta-analysis has shown that the FPC network's functional connectivity is lower in depressed patients compared to non-depressed individuals, which is associated with emotional regulation defects [39]. As known, the FPC network, particularly the lateral prefrontal cortex, is responsible for regulating cognitive and emotional tasks and plays a crucial role in regulating negative emotions [40–42]. Previous studies have demonstrated the functional imbalance of the lateral prefrontal cortex in depression patients, with reduced activity of the lateral prefrontal cortex, leading to emotional and cognitive changes [43, 44]. Therefore, the available evidence may reveal that disruption of the FPC network contributes to the negative effect on emotional regulation in individuals with depressive symptoms, which the same applies to StD individuals.

Our findings revealed significantly higher levels of salivary cortisol secretion in the StD adults, which was in line with previous findings on MDD. The increased cortisol level may be attributable to the high-level perceived stress, which was corroborated by the higher depression and stress scores in StD patients. It is plausible that high levels of stress exacerbate depression symptoms by triggering short-term increases in HPA axis activity and salivary cortisol secretion. More importantly, growing evidence supported that elevated cortisol levels could prospectively predict the subsequent onset of depression [10, 45, 46]. Herein, we combined the brain SC-FC coupling with cortisol levels to identify the subthreshold depression and reported greater predictive power (AUC 0.894, accuracy 85.71%) for subthreshold depression than other single models using only gray matter volume (AUC 0.69, accuracy 70.51%) [47] or resting functional connectivity (AUC 0.84, accuracy 80%) [48] in previous studies. Thus, these findings may indicate the robust predictive role of the combination of stress-related network activity and cortisol levels in the identification of subthreshold depression.

Limitations

There are still some limitations in this study. Firstly, it should be noted that the cross-sectional design of this study and its relatively small sample size might limit the generalizability of our findings and the ability to examine a longitudinal evolution of multiple levels of depressive symptomatology over time. However, we were able to preliminarily reveal the characteristics of SC-FC coupling in StD adults that could provide insights for future StD research. Secondly, we only measured the salivary cortisol level in the morning within an hour of waking up. It was suggested that measuring cortisol in saliva over three consecutive days and at different time points throughout the day could provide a more accurate picture of cortisol levels, as cortisol levels are affected by circadian rhythms and daily disturbances [49, 50]. Therefore, it could be considered for future research to measure the salivary cortisol levels more times to yield more comprehensive data to explore the relationship between cortisol secretion and subthreshold depression.

CONCLUSION

In conclusion, this study highlights the critical role of stress-related network SC-FC coupling in influencing depressive symptoms in StD adults. The combination of stress-related network SC-FC couplings with cortisol levels could hopefully help to discriminate StD from HC. These findings may provide a new perspective on the underlying mechanism of StD and may help to distinguish the subthreshold depressive states in the future.

DATA AVAILABILITY

The datasets used and/or analyzed during the current study are available from the corresponding author upon reasonable request.

REFERENCES

1. Cuijpers P, Smit F, van Straten A. Psychological treatments of subthreshold depression: a meta-analytic review. Acta Psychiatr Scand. 2007;115:434–41. https://doi.org/10.1111/j.1600-0447.2007.00998.x.
2. Sadek N, Bona J. Subsyndromal symptomatic depression: a new concept. Depress Anxiety. 2000;12:30–9. https://doi.org/10.1002/1520-6394(2000)12. 1<30::AID-DA4>3.0.CO;2-P.
3. Zhang R, Peng X, Song X, Long J, Wang C, Zhang C, et al. The prevalence and risk of developing major depression among individuals with subthreshold depression in the general population. Psychol Med. 2022:1–10. https://doi.org/10.1017/S0033291722000241.
4. Li H, Luo X, Ke X, Dai Q, Zheng W, Zhang C, et al. Major depressive disorder and suicide risk among adult outpatients at several general hospitals in a Chinese Han population. PLoS ONE. 2017;12:e0186143 https://doi.org/10.1371/journal.pone.0186143.
5. Park S, Hatim SA, Srisurapanont M, Chang SM, Liu CY, Bautista D, et al. The association of suicide risk with negative life events and social support according to gender in Asian patients with major depressive disorder. Psychiatry Res. 2015;228:277–82. https://doi.org/10.1016/j.psychres.2015.06.032.
6. Cristobal-Narvaez P, Haro JM, Koyanagi A. Longitudinal association between perceived stress and depression among community-dwelling older adults: findings from the Irish longitudinal study on ageing. J Affect Disord. 2022;299:457–62. https://doi.org/10.1016/j.jad.2021.12.041.
7. Russell G, Lightman S. The human stress response. Nat Rev Endocrinol. 2019;15:525–34. https://doi.org/10.1038/s41574-019-0228-0.
8. Juruena MF, Bocharova M, Agustini B, Young AH. Atypical depression and non-atypical depression: is hpa axis function a biomarker? A systematic review. J Affect Disord. 2018;233:45–67. https://doi.org/10.1016/j.jad.2017.09.052.
9. Verduijn J, Milaneschi Y, Schoevers RA, van Hemert AM, Beekman AT, Penninx BW. Pathophysiology of major depressive disorder: mechanisms involved in etiology are not associated with clinical progression. Transl Psychiatry. 2015;5:e649 https://doi.org/10.1038/tp.2015.137.

10. Zajkowska Z, Gullett N, Walsh A, Zonca V, Pedersen GA, Souza L, et al. Cortisol and development of depression in adolescence and young adulthood - a systematic review and meta-analysis. Psychoneuroendocrinology. 2022;136:105625 https://doi.org/10.1016/j.psyneuen.2021.105625.
11. Keller J, Gomez R, Williams G, Lembke A, Lazzeroni L, Murphy GJ, et al. Hpa axis in major depression: cortisol, clinical symptomatology, and genetic variation predict cognition. Mol Psychiatry. 2017;22:527–36. https://doi.org/10.1038/mp.2016.120.
12. Kuhnel A, Czisch M, Samann PG, Binder EB, Kroemer NB. Spatiotemporal dynamics of stress-induced network reconfigurations reflect negative affectivity. Biol Psychiatry. 2022;92:158–69. https://doi.org/10.1016/j.biopsych.2022.01.008.
13. Hwang JW, Egorova N, Yang XQ, Zhang WY, Chen J, Yang XY, et al. Subthreshold depression is associated with impaired resting-state functional connectivity of the cognitive control network. Transl Psychiatry. 2015;5:e683 https://doi.org/10.1038/tp.2015.174.
14. Hwang JW, Xin SC, Ou YM, Zhang WY, Liang YL, Chen J, et al. Enhanced default mode network connectivity with ventral striatum in subthreshold depression individuals. J Psychiatr Res. 2016;76:111–20. https://doi.org/10.1016/j.jpsychires.2016.02.005.
15. Vulser H, Lemaitre H, Artiges E, Miranda R, Penttilä J, Struve M, et al. Subthreshold depression and regional brain volumes in young community adolescents. J Am Acad Child Adolesc Psychiatry. 2015;54:832–40. https://doi.org/10.1016/j.jaac.2015.07.006.
16. Honey CJ, Sporns O, Cammoun L, Gigandet X, Thiran JP, Meuli R, et al. Predicting human resting-state functional connectivity from structural connectivity. Proc Natl Acad Sci USA. 2009;106:2035–40. https://doi.org/10.1073/pnas.0811168106.
17. Guerra-Carrillo B, Mackey AP, Bunge SA. Resting-state fMRI: a window into human brain plasticity. Neuroscientist. 2014;20:522–33. https://doi.org/10.1177/1073858414524442.
18. Dai Z, Lin Q, Li T, Wang X, Yuan H, Yu X, et al. Disrupted structural and functional brain networks in Alzheimer's disease. Neurobiol Aging. 2019;75:71–82. https://doi.org/10.1016/j.neurobiolaging.2018.11.005.
19. Zhang J, Zhang Y, Wang L, Sang L, Yang J, Yan R, et al. Disrupted structural and functional connectivity networks in ischemic stroke patients. Neuroscience. 2017;364:212–25. https://doi.org/10.1016/j.neuroscience.2017.09.009.
20. Zhang Z, Liao W, Chen H, Mantini D, Ding JR, Xu Q, et al. Altered functional-structural coupling of large-scale brain networks in idiopathic generalized epilepsy. Brain. 2011;134:2912–28. https://doi.org/10.1093/brain/awr223.
21. Liu X, He C, Fan D, Zhu Y, Zang F, Wang Q, et al. Disrupted rich-club network organization and individualized identification of patients with major depressive disorder. Prog Neuropsychopharmacol Biol Psychiatry. 2021;108:110074 https://doi.org/10.1016/j.pnpbp.2020.110074.
22. Zhang X, Shi Y, Fan T, Wang K, Zhan H, Wu W. Analysis of correlation between white matter changes and functional responses in post-stroke depression. Front Aging Neurosci. 2021;13:728622 https://doi.org/10.3389/fnagi.2021.728622.
23. Fotiadis P, Parkes L, Davis KA, Satterthwaite TD, Shinohara RT, Bassett DS. Structure-function coupling in macroscale human brain networks. Nat Rev Neurosci. 2024;25:688–704. https://doi.org/10.1038/s41583-024-00846-6.
24. Ma J, Liu F, Yang B, Xue K, Wang P, Zhou J, et al. Selective aberrant functional-structural coupling of multiscale brain networks in subcortical vascular mild cognitive impairment. Neurosci Bull. 2021;37:287–97. https://doi.org/10.1007/s12264-020-00580-w.
25. Wang XM, Ma HY, Zhong J, Huang XJ, Yang CJ, Sheng DF, et al. A chinese adaptation of six items, self-report Hamilton depression scale: factor structure and psychometric properties. Asian J Psychiatr. 2022;73:103104 https://doi.org/10.1016/j.ajp.2022.103104.
26. Spitzer RL, Kroenke K, Williams JB, Löwe B. A brief measure for assessing generalized anxiety disorder: the gad-7. Arch Intern Med. 2006;166:1092–7. https://doi.org/10.1001/archinte.166.10.1092.
27. Yokokura A, Silva A, Fernandes J, Del-Ben CM, Figueiredo FP, Barbieri MA, et al. Perceived stress scale: confirmatory factor analysis of the pss14 and pss10 versions in two samples of pregnant women from the Brisa cohort. Cad Saude Publica. 2017;33:e00184615 https://doi.org/10.1590/0102-311X00184615.
28. Schaefer A, Kong R, Gordon EM, Laumann TO, Zuo XN, Holmes AJ, et al. Local-global parcellation of the human cerebral cortex from intrinsic functional connectivity MRI. Cereb Cortex. 2018;28:3095–114. https://doi.org/10.1093/cercor/bhx179.
29. Achard S, Bullmore E. Efficiency and cost of economical brain functional networks. PLoS Comput Biol. 2007;3:e17 https://doi.org/10.1371/journal.pcbi.0030017.
30. Pruessner M, Hellhammer DH, Pruessner JC, Lupien SJ. Self-reported depressive symptoms and stress levels in healthy young men: associations with the cortisol response to awakening. Psychosom Med. 2003;65:92–9. https://doi.org/10.1097/01.psy.0000040950.22044.10.
31. Heymans MW, Twisk J. Handling missing data in clinical research. J Clin Epidemiol. 2022;151:185–8. https://doi.org/10.1016/j.jclinepi.2022.08.016.
32. Chan SY, Ong ZY, Ngoh ZM, Chong YS, Zhou JH, Fortier MV, et al. Structure-function coupling within the reward network in preschool children predicts executive functioning in later childhood. Dev Cogn Neurosci. 2022;55:101107 https://doi.org/10.1016/j.dcn.2022.101107.
33. Sarwar T, Tian Y, Yeo B, Ramamohanarao K, Zalesky A. Structure-function coupling in the human connectome: a machine learning approach. Neuroimage. 2021;226:117609 https://doi.org/10.1016/j.neuroimage.2020.117609.
34. Satpute AB, Lindquist KA. The default mode network's role in discrete emotion. Trends Cogn Sci. 2019;23:851–64. https://doi.org/10.1016/j.tics.2019.07.003.
35. Rzepa E, Mccabe C. Anhedonia and depression severity dissociated by dmpfc resting-state functional connectivity in adolescents. J Psychopharmacol. 2018;32:1067–74. https://doi.org/10.1177/0269881118799935.
36. Zhu Z, Wang Y, Lau W, Wei X, Liu Y, Huang R, et al. Hyperconnectivity between the posterior cingulate and middle frontal and temporal gyrus in depression: based on functional connectivity meta-analyses. Brain Imaging Behav. 2022;16:1538–51. https://doi.org/10.1007/s11682-022-00628-7.
37. Wang S, Tepfer LJ, Taren AA, Smith DV. Functional parcellation of the default mode network: a large-scale meta-analysis. Sci Rep. 2020;10:16096 https://doi.org/10.1038/s41598-020-72317-8.
38. Yang R, Gao C, Wu X, Yang J, Li S, Cheng H. Decreased functional connectivity to posterior cingulate cortex in major depressive disorder. Psychiatry Res Neuroimaging. 2016;255:15–23. https://doi.org/10.1016/j.pscychresns.2016.07.010.
39. Kaiser RH, Andrews-Hanna JR, Wager TD, Pizzagalli DA. Large-scale network dysfunction in major depressive disorder: a meta-analysis of resting-state functional connectivity. JAMA Psychiatry. 2015;72:603–11. https://doi.org/10.1001/jamapsychiatry.2015.0071.
40. Davidson RJ, Putnam KM, Larson CL. Dysfunction in the neural circuitry of emotion regulation-a possible prelude to violence. Science. 2000;289:591–4. https://doi.org/10.1126/science.289.5479.591.
41. White LK, Makhoul W, Teferi M, Sheline YI, Balderston NL. The role of dlPFC laterality in the expression and regulation of anxiety. Neuropharmacology. 2023;224:109355 https://doi.org/10.1016/j.neuropharm.2022.109355.
42. Zhao W, Zhang X, Zhou X, Song X, Zhang Z, Xu L, et al. Depression mediates the association between insula-frontal functional connectivity and social interaction anxiety. Hum Brain Mapp. 2022;43:4266–73. https://doi.org/10.1002/hbm.25952.
43. Mayberg HS, Brannan SK, Tekell JL, Silva JA, Mahurin RK, Mcginnis S, et al. Regional metabolic effects of fluoxetine in major depression: serial changes and relationship to clinical response. Biol Psychiatry. 2000;48:830–43. https://doi.org/10.1016/s0006-3223(00)01036-2.
44. Zhang X, Zhang R, Lv L, Qi X, Shi J, Xie S. Correlation between cognitive deficits and dorsolateral prefrontal cortex functional connectivity in first-episode depression. J Affect Disord. 2022;312:152–8. https://doi.org/10.1016/j.jad.2022.06.024.
45. Stetler C, Miller GE. Depression and hypothalamic-pituitary-adrenal activation: a quantitative summary of four decades of research. Psychosom Med. 2011;73:114–26. https://doi.org/10.1097/PSY.0b013e31820ad12b.
46. Vrshek-Schallhorn S, Doane LD, Mineka S, Zinbarg RE, Craske MG, Adam EK. The cortisol awakening response predicts major depression: predictive stability over a 4-year follow-up and effect of depression history. Psychol Med. 2013;43:483–93. https://doi.org/10.1017/S0033291712001213.
47. Ma H, Zhang D, Sun D, Wang H, Yang J. Gray and white matter structural examination for diagnosis of major depressive disorder and subthreshold depression in adolescents and young adults: a preliminary radiomics analysis. BMC Med Imaging. 2022;22:164 https://doi.org/10.1186/s12880-022-00892-5.
48. Sato Y, Okada G, Yokoyama S, Ichikawa N, Takamura M, Mitsuyama Y, et al. Resting-state functional connectivity disruption between the left and right pallidum as a biomarker for subthreshold depression. Sci Rep. 2023;13:6349 https://doi.org/10.1038/s41598-023-33077-3.
49. Chojnowska S, Ptaszyńska-Sarosiek I, Kępka A, Knaś M, Waszkiewicz N. Salivary biomarkers of stress, anxiety and depression. J Clin Med. 2021;10. https://doi.org/10.3390/jcm10030517.
50. Yonekura T, Takeda K, Shetty V, Yamaguchi M. Relationship between salivary cortisol and depression in adolescent survivors of a major natural disaster. J Physiol Sci. 2014;64:261–7. https://doi.org/10.1007/s12576-014-0315-x.

AUTHOR CONTRIBUTIONS

HYZ, ZBR, and LZH contributed equally to this article. HYZ was responsible for the data curation, formal analysis, methodology, and writing the manuscript; ZBR and LZH were responsible for the data curation, formal analysis, and writing the

manuscript; HYD and SJ were responsible for the data curation and writing the manuscript. WJS was responsible for the study conceptualization, funding acquisition, resources, manuscript review, and editing. All authors contributed to the writing and approved the final version of the manuscript.

FUNDING

This study was supported by the National Natural Science Foundation of China (No. 8247153749), 2022 Research Project of Chinese Association of Rehabilitation Medicine (No. KFKT-2022-013), 2022 Major Scientific and Technological Innovation Project of Fujian University of Traditional Chinese Medicine (No. XJB2022006), Young Scientific and Technological Innovative Talents Training Project of Fujian University of Traditional Chinese Medicine (No. XQC2023004).

COMPETING INTERESTS

All authors declared no competing interests.

ADDITIONAL INFORMATION

Supplementary information The online version contains supplementary material available at https://doi.org/10.1038/s41398-024-03210-5.

Correspondence and requests for materials should be addressed to Jingsong Wu.